Available online at www.sciencedirect.com

SCIENCE DIRECT®

ELSEVIER

International Journal of Heat and Mass Transfer 48 (2005) 2150–2158

International Journal of HEAT and MASS TRANSFER

www.elsevier.com/locate/ijhmt

Thermal conductivity bounds for isotropic, porous materials

James K. Carson [a,*], Simon J. Lovatt [a], David J. Tanner [b], Andrew C. Cleland [c]

[a] *AgResearch Ltd., Private Bag 3123, Hamilton, New Zealand*
[b] *Food Science Australia, P.O. Box 52, North Ryde, NSW 1670 Sydney, Australia*
[c] *IPENZ, P.O. Box 12-241, Wellington, New Zealand*

Received 30 July 2004; received in revised form 31 December 2004
Available online 8 March 2005

Abstract

To avoid potential misapplication of effective thermal conductivity models, materials that may be described as 'porous' should be divided into two classes; 'internal porosity' materials which have bubbles/pores suspended within a continuous condensed phase (e.g. sponges, foams, honeycombs), and 'external porosity' materials which include granular/particulate materials. It is proposed that the effective thermal conductivity region bounded by the Hashin–Shtrikman bounds may be divided into internal porosity and external porosity regions by the Effective Medium Theory (EMT) equation. The use of the Hashin–Shtrikman and EMT equations as porosity bounds was supported by experimental data from the literature.

Keywords: Effective thermal conductivity; Porous materials

---

1. Introduction

The prediction of the thermal conductivity of heterogeneous or composite materials comprises a significant portion of the heat transfer literature, and a significant number of effective thermal conductivity models have been proposed [1–4]. Many of the models that have been proposed are either purely empirical or are theoretically based but highly specific to a given material. Some theoretically based models may have wider applicability, but their convenience of use is limited by the inclusion of parameters whose values must be determined empirically. Several researchers have proposed generic models by deriving a set of equations, usually based on a conceptual 'parent' model that is modified to account for variations in composition and structure, although some of these still include empirical parameters [5–8]. However, even a cursory glance of the literature will reveal that new models continue to appear—which suggests that, to-date, no single model or prediction procedure has been found with universal applicability.

Much of the effective thermal conductivity literature is concerned with porous materials; however, the term 'porous' itself may be the cause of some confusion. In some situations it refers to granular or particulate materials, in which the void volume may be occupied by either liquid or gaseous components; alternatively, it may refer to a material having a continuous solid matrix that contains pores/bubbles, which may be isolated or interconnected. Problems may arise when a model that has been shown to work well for one type of porous material is assumed to be applicable to another type,

---

[*] Corresponding author. Tel.: +64 7 838 5372; fax: +64 7 838 5625.

E-mail address: james.carson@agresearch.co.nz (J.K. Carson).

0017-9310/$ - see front matter © 2005 Elsevier Ltd. All rights reserved.
doi:10.1016/j.ijheatmasstransfer.2004.12.032

Nomenclature

A,B,C,D	constants in Eq. (10)
b	magnitude of temperature gradient (K m^{-1})
k	thermal conductivity (W m^{-1} K^{-1})
n	number of small spheres
p	probability function (Eq. (18))
q	heat flux (W m^{-2})
r	radial coordinate
R	sphere/cylinder radius (m)
T	temperature (K)
v	volume fraction of material component
V	volume (m^3)
w	number of components
z	axial coordinate

Greek symbols

ε	porosity
θ	latitudinal spherical polar coordinate
ϕ	longitudinal spherical polar coordinate

Subscripts

1	component 1
2	component 2
cont	continuous phase
disp	dispersed (discontinuous) phase
e	effective
i	component *i*
m	continuous medium
s	sphere
solid	solid phase

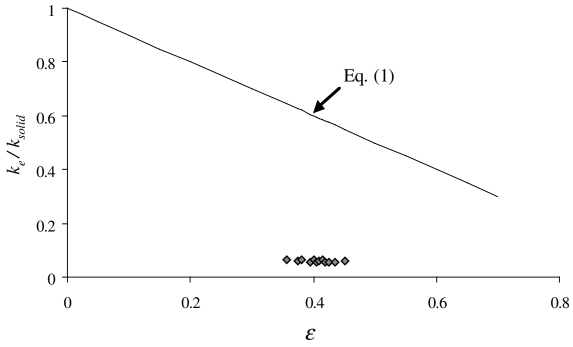

Fig. 1. Predictions of Francl's model Eq. (1) with effective thermal conductivity data for loose sand, $k_{\text{solid}}/k_{\text{air}} = 166$ [10].

simply because both materials have been described as 'porous'. For example, Francl's model (Eq. (1)) has been shown to be effective for a certain porous material [9];

$$k_{\text{e}} = k_{\text{solid}}(1 - \varepsilon) \tag{1}$$

however, if it were to be applied to a granular material such as sand, the thermal conductivity predicted by Eq. (1) would be erroneous by several orders of magnitude (Fig. 1, thermal conductivity data from [10]).

In this paper, it is proposed that this problem may be clarified by distinguishing 'internal porosity' from 'external porosity', and that thermal conductivity bounds which depend only on the thermal conductivities and volume fractions of the material's components may be defined for each class of porous material. The analysis is limited to steady-state conduction heat transfer, and to materials that may be considered isotropic on the macroscopic scale.

Although the focus of this paper is on porous materials, the analysis could be applied to any isotropic, two-component, heterogeneous material, since the models involved do not require the specification of components as being either solid or fluid.

2. Optimal heat conduction pathways

Consider the theoretical material depicted in Fig. 2a and b (simulated using the finite element software package *FlexPDE*™). In both cases, one component is dispersed as circular inclusions within a continuous medium of the other component. Both are subjected to a steady-state temperature gradient from the top to the bottom of the figures. However, the thermal conductivity of the circles (i.e. the dispersed phase) of the material in Fig. 2a is less than the thermal conductivity of the surrounding material (continuous phase), while the opposite is true for the material in Fig. 2b. The arrows represent heat flux vectors **q**, where:

$$\mathbf{q} = -\mathbf{k}\,\text{grad}(\mathbf{T}) \tag{2}$$

Based on the magnitudes and directions of the heat flux vectors shown in Fig. 2a and b, the following significant inferences can be drawn:

- the optimal heat conduction pathway is dependent on whether the thermal conductivity of the dispersed phase is higher or lower than the thermal conductivity of the continuous phase
- when $k_{\text{cont}} > k_{\text{disp}}$ the heat flow essentially avoids the dispersed phase
- when $k_{\text{cont}} < k_{\text{disp}}$ the heat flow involves the dispersed phase as much as possible.

Although represented simplistically in two dimensions in Fig. 2a and b, a similar set of conclusions may

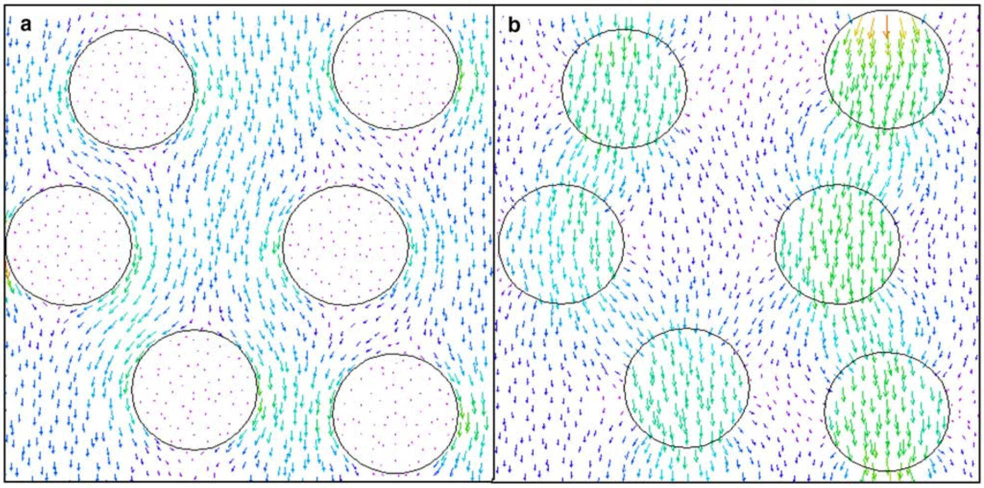

Fig. 2. Heat flux vectors for a dispersion of spheres in a continuous medium (a) with $k_{\mathrm{cont}} > k_{\mathrm{disp}}$; (b) with $k_{\mathrm{cont}} < k_{\mathrm{disp}}$.

be drawn intuitively for most isotropic, porous structures. For materials in which the lower conductivity component is dispersed in pores/bubbles within a higher-conductivity continuous medium (such as a foam or a sponge), the optimal heat transfer pathway is represented by the scenario depicted in Fig. 2a (i.e. heat flow avoiding air bubbles). Conversely, for particulate materials surrounded by a lower conductivity phase, the optimal heat transfer pathway is represented by the scenario depicted in Fig. 2b (i.e. heat flow through particles where possible). Hence, due to the different optimal conduction pathways, a foam and a particulate material will not necessarily have the same effective thermal conductivities simply because they may have identical void fractions and component thermal conductivities. This distinction between porous materials according to the optimal heat transfer pathways, as described above, is seldom made in the effective thermal conductivity literature.

It is therefore convenient to introduce terms to distinguish between these two basic types of porous materials. Particulate-type materials in which air (for instance) comprises a continuous phase will be referred to as 'external porosity' materials, and materials such as foams, sponges, and honeycomb-structures in which air (for instance) is dispersed within a continuous condensed phase (i.e. solid or solid/immobilised-liquid) will be referred to as 'internal porosity' materials.

3. Thermal conductivity bounds for internal and external porosity materials

The Series and Parallel models serve as lower and upper bounds respectively for the effective conductivity of heterogeneous materials, provided conduction is the only mechanism of heat transfer involved (sometimes referred to as the Wiener bounds) [11]:

$$\text{Series model:} \quad k_e = \frac{1}{(1-v_2)/k_1 + v_2/k_2} \tag{3}$$

$$\text{Parallel model:} \quad k_e = (1-v_2)k_1 + v_2 k_2 \tag{4}$$

Hashin and Shtrikman [12] derived effective conductivity bounds that were the best (i.e. narrowest) possible bounds for macroscopically homogeneous, isotropic, two-phase materials that could be derived from the components' volume fractions and conductivities. The Hashin–Shtrikman bounds always lie within the Series–Parallel bounds, regardless of the components' volume fractions or thermal conductivities.

Although arrived at by different lines of reasoning, the equations presented by Hashin and Shtrikman as conductivity bounds were mathematically equivalent to the two forms of the well-known Maxwell–Eucken model [12].

Maxwell–Eucken 1:

$$k_e = k_1 \frac{2k_1 + k_2 - 2(k_1 - k_2)v_2}{2k_1 + k_2 + (k_1 - k_2)v_2} \tag{5}$$

Maxwell–Eucken 2:

$$k_e = k_2 \frac{2k_2 + k_1 - 2(k_2 - k_1)(1 - v_2)}{2k_2 + k_1 + (k_2 - k_1)(1 - v_2)} \tag{6}$$

This apparent coincidence can be explained intuitively by returning to the optimal-heat-conduction-pathway analysis described above. An assumption of Maxwell's model was that the inclusions of the dispersed

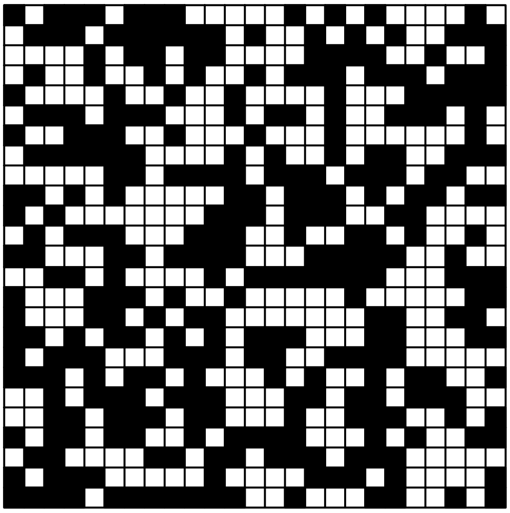

Fig. 3. Schematic diagram of a material made up of a random dispersion of two components.

phase (whether particles or bubbles) did not come into contact with neighbouring inclusions [13]. This meant that the dispersed phase could never form continuous conduction pathways, and hence, from a heat transfer perspective, Maxwell's model had a 'maximum bias' towards the continuous phase.

Consider the structure depicted in Fig. 3 which represents a heterogeneous material in which the two components are distributed randomly, with neither phase being necessarily continuous or dispersed. Either component may form continuous heat conduction pathways, depending on the relative amounts of the components, and therefore this structure is 'unbiased' towards its components. The effective conductivity of this type of structure is modelled well by the Effective Medium Theory (EMT) equation [14,15]:

$$(1-v_2)\frac{k_1-k_\mathrm{e}}{k_1+2k_\mathrm{e}}+v_2\frac{k_2-k_\mathrm{e}}{k_2+2k_\mathrm{e}}=0 \tag{7}$$

which may be rewritten to be explicit for k_e:

$$k_\mathrm{e}=1/4\left((3v_2-1)k_2+[3(1-v_2)-1]k_1 + \sqrt{[(3v_2-1)k_2+(3\{1-v_2\}-1)k_1]^2+8k_1k_2}\right) \tag{8}$$

The concept of conduction 'bias' towards components can also be seen in the derivation of the Maxwell–Eucken and EMT models. Both may be derived from the solution of Laplace's equation applied to a single sphere of radius R and conductivity k_s surrounded by a continuous medium of conductivity k_m, and subjected to a steady-state temperature gradient in the direction of the z-axis, as depicted in Fig. 4.

If $k_\mathrm{s} \neq k_\mathrm{m}$, a localised distortion to the spatial temperature distribution around the sphere will result.

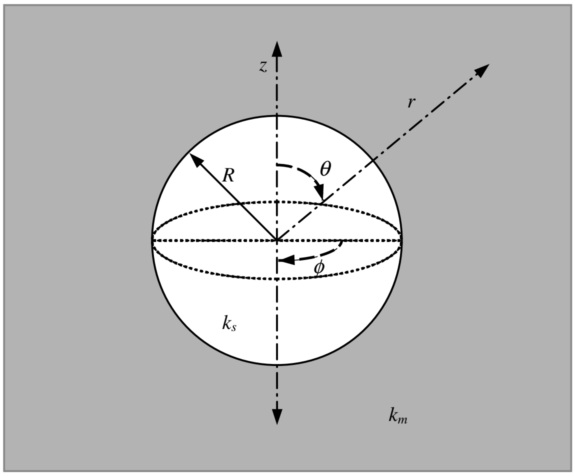

Fig. 4. Single sphere of conductivity k_s contained within a continuous medium of conductivity k_m.

Under steady-state conditions the temperature distribution within a region of constant thermal conductivity is governed by Laplace's Equation, shown below in spherical polar coordinates:

$$\frac{1}{r^2}\frac{\partial}{\partial r}\left(r^2\frac{\partial T}{\partial r}\right)+\frac{1}{r^2\sin\theta}\frac{\partial}{\partial\theta}\left(\sin\theta\frac{\partial T}{\partial\theta}\right)+\frac{1}{r^2\sin^2\theta}\frac{\partial^2 T}{\partial\phi^2}=0 \tag{9}$$

Taking the centre of the sphere as the origin, and assuming symmetry about the z-axis such that T is independent of ϕ, a general solution of Eq. (9) is:

$$T=A+\frac{B}{r}+Cr\cos\theta+\frac{D}{r^2}\cos\theta \tag{10}$$

where A, B, C and D must be determined from the following boundary conditions:

at $r=0 \quad T_\mathrm{s}\neq\infty$

at $r=R \quad k_\mathrm{s}\frac{\partial T_\mathrm{s}}{\partial r}=k_\mathrm{m}\frac{\partial T_\mathrm{m}}{\partial r}$ and $\frac{\partial T_\mathrm{s}}{\partial\theta}=\frac{\partial T_\mathrm{m}}{\partial\theta}$

at $r\gg R \quad T_\mathrm{m}=bz=br\cos\theta$

The constant b (K m^{-1}) is the magnitude of the temperature gradient in the continuous medium. Using the boundary conditions to substitute for A, B, C and D in Eq. (10) yields:

$$T_\mathrm{s}=b\frac{3k_\mathrm{m}}{k_\mathrm{s}+k_\mathrm{m}}r\cos\theta \tag{11}$$

for the temperature distribution within the sphere, and:

$$T_\mathrm{m}=br\cos\theta-bR^3\frac{k_\mathrm{s}-k_\mathrm{m}}{k_\mathrm{s}+2k_\mathrm{m}}\frac{\cos\theta}{r^2} \tag{12}$$

for the external temperature distribution.

The difference between the Maxwell and EMT models arises from the different assumptions made in order to derive expressions for situations involving multiple inclusions, based on Eq. (12). Maxwell [13] considered the situation where n small spheres of radius R_2 and conductivity k_2 were contained within a single larger sphere R_1 with conductivity k_1 such that the local distortions to the temperature distributions around the smaller spheres did not affect their neighbours. From Eq. (12):

$$T_{\mathrm{m}} = br\cos\theta - bnR_2^3\frac{k_2 - k_1}{k_2 + 2k_1}\frac{\cos\theta}{r^2} \tag{13}$$

The volume fraction of the small spheres within the volume of the larger sphere was:

$$v_2 = \frac{nR_2^3}{R_1^3} \tag{14}$$

and so Eq. (13) became:

$$T_{\mathrm{m}} = br\cos\theta - bv_2R_1^3\frac{k_2 - k_1}{k_2 + 2k_1}\frac{\cos\theta}{r^2} \tag{15}$$

If the large sphere had been filled with a material having an effective conductivity k_{e}, Eq. (12) would have become:

$$T_{\mathrm{m}} = br\cos\theta - bR_1^3\frac{k_{\mathrm{e}} - k_1}{k_{\mathrm{e}} + 2k_1}\frac{\cos\theta}{r^2} \tag{16}$$

In order for Eqs. (15) and (16) to produce the same result:

$$\frac{k_{\mathrm{e}} - k_1}{k_{\mathrm{e}} + 2k_1} = v_2\frac{k_2 - k_1}{k_2 + 2k_1} \tag{17}$$

which, when rearranged, is identical to Eq. (5).

By contrast, the EMT model assumed that for a completely random distribution of components the effect of local distortions to the temperature distribution caused by individual inclusions could be averaged such that over a sufficiently large volume (V) the temperature distribution within the material could be approximated by a material having a uniform temperature distribution and thermal conductivity k_{e} [16]. This assumption required that the net effect from the second term on the right hand side of Eq. (12) must be zero, i.e.:

$$\int_V \left(\frac{k_i - k_{\mathrm{e}}}{k_i + 2k_{\mathrm{e}}}\right) p(k_i)\,\mathrm{d}k = 0 \tag{18}$$

where $p(k_i)\,\mathrm{d}k$ is the probability that the component at an arbitrary location within the heterogeneous material has a thermal conductivity equal to k_i. For a random distribution of components, this probability is directly proportional to the volume fraction (v_i) of the component, hence for w components:

$$\sum_{i=1}^{w} v_i\frac{k_i - k_{\mathrm{e}}}{k_i + 2k_{\mathrm{e}}} = 0 \tag{19}$$

Eq. (7) is the two-component form of Eq. (19).

Fig. 5 shows plots of relative effective thermal conductivities (k_{e}/k_1) for the Series, Parallel, Maxwell–

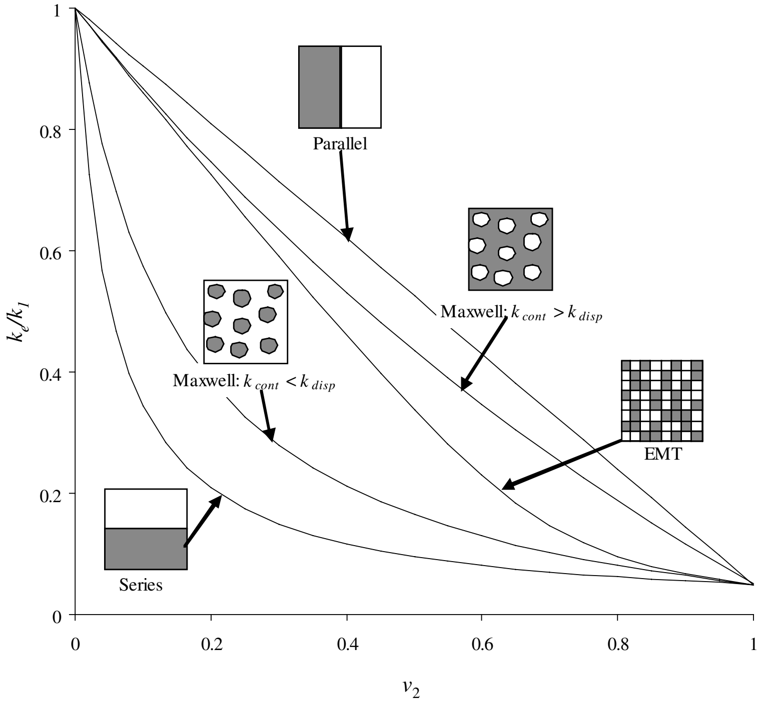

Fig. 5. Plot of Eqs. (3)–(7) with schematic representations of the structure assumed by each model.

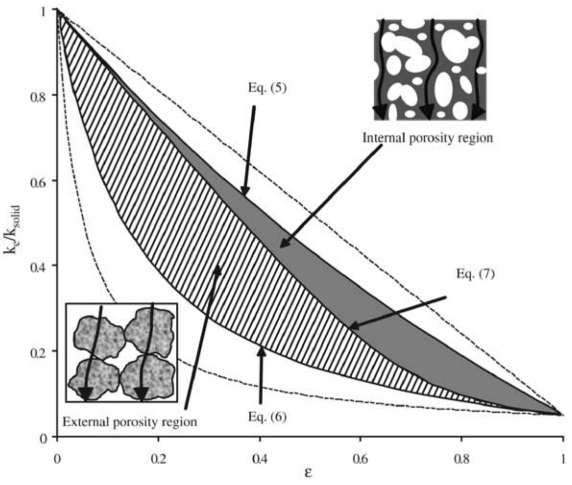

Fig. 6. 'Internal porosity' region bounded above by Eq. (5) and below by Eq. (7); 'external porosity' region bounded above by Eq. (7) and below by Eq. (6).

Eucken and EMT models for a two-component material with $k_1/k_2 = 20$, over the full range of composition. A schematic of the material structures assumed by each model is also shown.

External porosity materials were identified above as those in which the gaseous component forms continuous conduction pathways, and therefore the effective conductivity of an external porosity material would be expected to be bounded below by the form of the Maxwell–Eucken model in which the gaseous component is the continuous phase (i.e. the lower Hashin–Shtrikman bound), and above by EMT model. Similarly, since internal porosity materials are those in which the condensed phase forms continuous conduction pathways, the effective conductivity of an internal porosity material would be expected to be bounded above by the form of the Maxwell–Eucken model in which the condensed phase is continuous (i.e. the upper Hashin–Shtrikman bound), and below by the EMT model. Hence the region between the Hashin–Shtrikman bounds may be divided into an "internal porosity region" and an "external porosity region", as illustrated by Fig. 6.

4. Testing the bounds

In order to test the proposed thermal conductivity bounds, published experimental thermal conductivity data were plotted in charts similar to Figs. 5 and 6, with

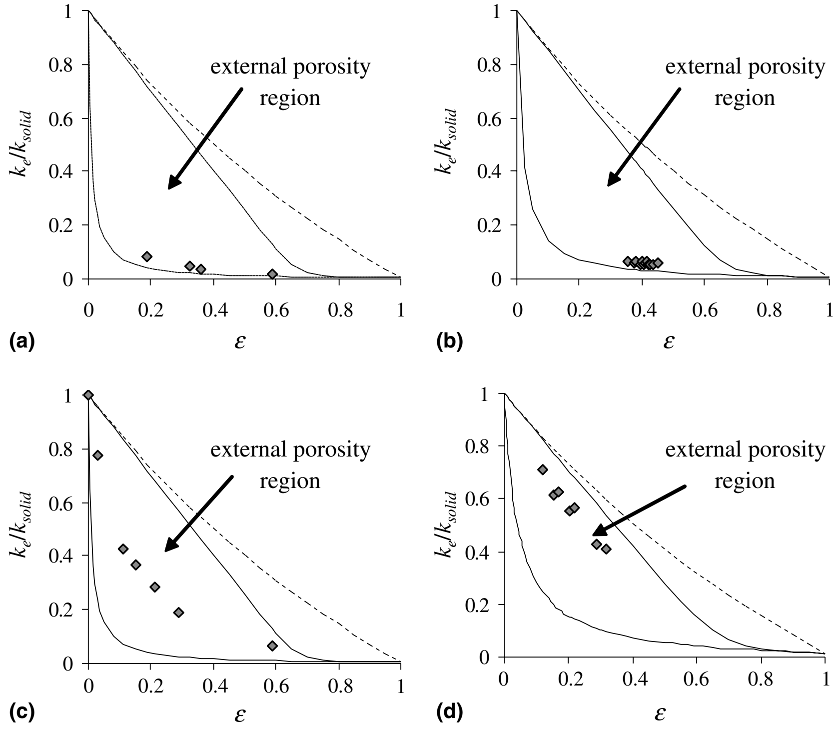

Fig. 7. Experimental thermal conductivity for porous materials plotted with the proposed 'porosity bounds'; (a) dry sand, $k_{\mathrm{solid}}/k_{\mathrm{air}} = 348$ [17], (b) dry sand, $k_{\mathrm{solid}}/k_{\mathrm{air}} = 166$ [10], (c) porous rock, $k_{\mathrm{solid}}/k_{\mathrm{air}} = 348$ [18], (d) sandstone, $k_{\mathrm{solid}}/k_{\mathrm{air}} = 70$ [19].

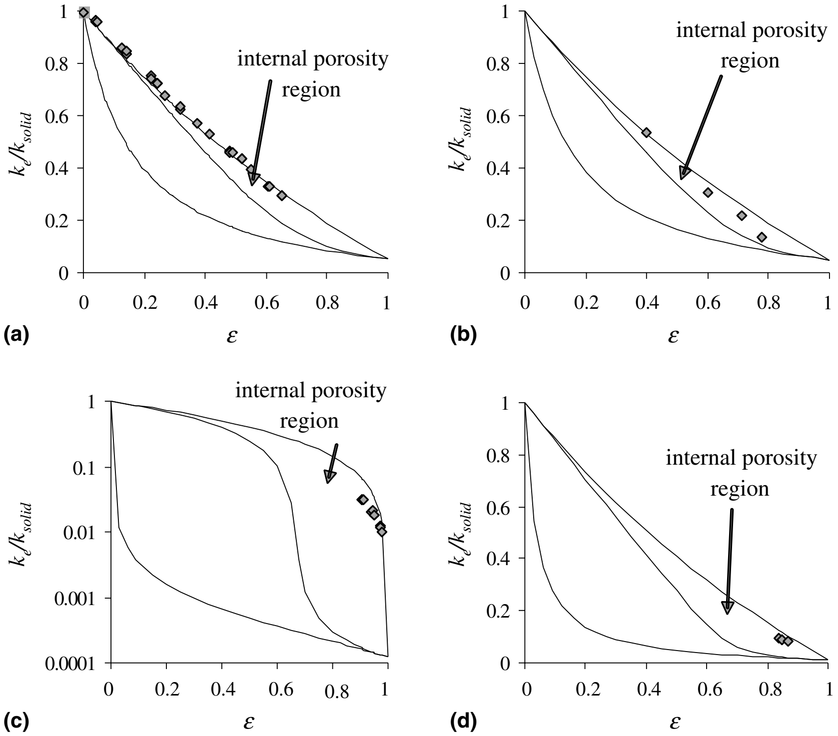

Fig. 8. Experimental thermal conductivity for porous materials plotted with the proposed 'porosity bounds': (a) porous food gel, $k_{\text{solid}}/k_{\text{air}} = 19$ [20], (b) aqueous alginate/saponin foam, $k_{\text{solid}}/k_{\text{air}} = 20$ (electrical conductivity) [7], (c) metallic foam, $k_{\text{solid}}/k_{\text{air}} = 8200$ [21], (d) cellular ceramic, $k_{\text{solid}}/k_{\text{air}} = 81$ [22].

relative thermal conductivity on the ordinate axis, and porosity on the abscissa axis. Data were chosen that were measured near to room temperature, to minimise the possible influence of radiation in the gaseous phase. Fig. 7a and b shows data for dry, loose sand [10,17] along with the porosity bounds, while Fig. 7c and d show similar plots for consolidated sands (sandstone) [18,19]. Consistent with the discussion above, all these data for granular-type materials lay within the "external porosity region", i.e. between the lower Hashin–Shtrikman bound and the EMT-model (cf. Fig. 6).

Fig. 8a–d show similar plots for a porous food gel [20], an aqueous alginate/saponin foam [7], a metallic foam [21] and a cellular ceramic [22] respectively. Consistent with the discussion above, all these data for foam-type materials lay within the "internal porosity region", i.e. between the upper Hashin–Shtrikman bound and the EMT-model (cf. Fig. 6).

5. Difficulties with identifying continuous and dispersed phases

In some materials, the identification of continuous and dispersed phases is self-evident; however, while the terms 'continuous phase' and 'dispersed phase' appear frequently in the effective thermal conductivity literature, these terms lack clear definitions, and ambiguities may arise from different interpretations of the words 'continuous' and 'dispersed'. Ultimately the material structure may need to be analysed in terms of its optimum heat transfer pathways in order to avoid potential confusion.

For example, the relatively low porosities of sandstone might suggest that air comprised the dispersed phase, and it might therefore be expected that sandstone was an internal porosity material. However, Fig. 7d shows that the data actually lie in the external porosity region, which, at face value, would appear to contradict the discussion so far.

Fig. 9 shows a schematic diagram of a lump of consolidated granular material such as sandstone, which is made up of discrete particles that have been compacted to form a larger solid (compare with Fig. 11 of [19]). Because the particles are packed tightly with smaller particles filling the interstices between larger particles, each individual particle is held in place and the overall mechanical properties are essentially those of a single solid. However, although the consolidated material does have physical continuity, Fig. 11 shows that the proportion of the

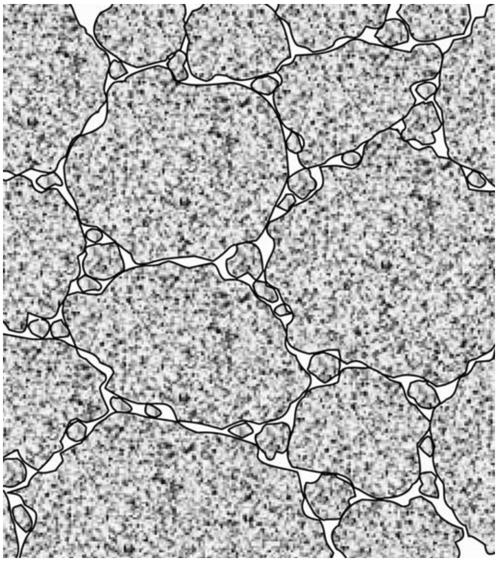

Fig. 9. Schematic diagram of consolidated granular material (e.g. sandstone).

surface of each particle that is in direct contact with neighbouring particles is small, and so while there is sufficient contact for each particle to be held in a fixed position relative to its neighbours, the heat conduction is inhibited by the low proportion of surface area that is in intimate contact with neighbouring particles (i.e. there is significant internal contact resistance). Hence, although it occupies only a small proportion of the total space, the gaseous phase behaves as the 'continuous phase' from an effective thermal conductivity perspective, and the sandstone is actually an external porosity material. The 'continuous phase' and 'dispersed phase' of a material should therefore be defined and identified from a heat transfer perspective rather than from a physical or mechanical perspective when its effective thermal conductivity is at issue.

6. Implications of the proposed bounds

If conduction is the only heat transfer mechanism involved, it may reasonably be assumed that the thermal conductivity of a porous material will lie between the Wiener bounds; if the material is isotropic on a macroscopic scale, the range of possible thermal conductivity is further reduced by the Hashin–Shtrikman bounds. Using the bounds proposed above, the range of possible thermal conductivities may be reduced again based on whether the material has internal or external porosity.

Fig. 6 shows that the external porosity region is larger than the internal porosity region, and this is true for any value of k_1/k_2. The implication of this observation is that there is inherently more uncertainty in the prediction of the thermal conductivities of external porosity materials than there is for internal porosity materials, as has been suggested previously [24,25]. This may be explained by returning to the analysis of heat conduction pathways. For internal porosity materials, the majority of the heat flow is through the condensed phase even if this phase comprises significantly less than 10% of the material's volume [21,26], and so it is not influenced greatly by the extent of thermal contact between the pores. However, for external porosity materials the heat transfer pathways are strongly dependent on the extent/quality of thermal contact between neighbouring particles. Since thermal contact is affected by the shape and distribution of the inclusions, there is a much greater level of randomness involved, and hence much more uncertainty in predicting the thermal conductivity.

Since the extent/quality of thermal contact between particles is so influential, models that are functions only of the components' volume fractions and conductivities will have limited applicability, and more versatile models will require some measure of thermal contact [27]. However, other than for regular arrangements of regularly shaped particles, it has proven difficult to predict the value of this variable. Kunii and Smith [28] suggested that the extent of thermal contact between neighbouring particles was a material-specific property, and Nozad et al. [29] found that it was difficult to determine its value other than by empirical means, which explains why most generic models include at least one empirical parameter.

However, Figs. 5 and 6 show that for low concentrations of the dispersed phase (i.e. $v_{\mathrm{disp}} < 0.2$), the predictions of the Maxwell and EMT models are almost identical, which suggests that the interactions between individual inclusions of the dispersed phase are negligible below this threshold. Hence, the thermal conductivity of this type of material may be predicted accurately based on the components' volume fractions and conductivities alone, regardless of whether the dispersed phase has a higher or lower conductivity than the continuous phase, and either of the EMT or Maxwell models would provide accurate predictions.

7. Conclusions

- Isotropic porous materials may be divided into two classes: internal porosity materials are materials in which the optimal heat transfer pathway is through the continuous phase, while external porosity materials are those in which the optimal heat conduction pathway is through the dispersed phase.
- A model that accurately predicts the effective thermal conductivity of internal porosity materials will not necessarily be applicable to external porosity materials or vice versa.

- It was proposed that the effective thermal conductivity of internal porosity materials is bounded above by the Maxwell–Eucken equation with the lower-conductivity material as the dispersed phase, and below by the EMT equation; and that the effective thermal conductivity of external porosity materials is bounded above by the EMT equation, and below by the Maxwell–Eucken equation with the lower-conductivity material as the continuous phase.
- The use of these equations as thermal conductivity bounds was supported by experimental data from the literature.
- The bounds support conclusions from previous studies that suggested there was inherently greater uncertainty involved with predicting the effective thermal conductivity of external porosity materials than there is with internal porosity materials.

Acknowledgment

This work was funded by the *Foundation for Research, Science & Technology* (New Zealand) as part of Objective 2 of Contract MRI 801.

References

[1] R.C. Progelhof, J.L. Throne, R.R. Reutsch, Methods for predicting the thermal conductivity of composite systems: A review, Polym. Eng. Sci. 16 (1976) 615–625.

[2] M.S. Rahman, Food Properties Handbook, CRC Press, Boca Raton, 1995 (Chapter 5).

[3] P. Cheng, H. Chin-Tsau, Heat conduction, in: D.B. Ingham, I. Pop (Eds.), Transport Phenomena in Porous Media, Pergamon press, 1998, pp. 57–76.

[4] E. Tsotsas, H. Martin, Thermal conductivity of packed beds: A review, Chem. Eng. Process. 22 (1987) 19–37.

[5] D.A.G. Bruggeman, Calculation of different physical constants of heterogeneous substances: I. Dielectric constant and conductivity of media of isotropic substances (Berechnung verschiedener physikalischer Konstanten von heterogenen Substanzen: I. Dielektrizitätskonstanten und Leitfähigkeiten der Mischkörper aus isotropen Substanzen), Ann. Phys. 24 (1935) 636–664.

[6] E. Behrens, Thermal conductivities of composite materials, J. Compos. Mater. 2 (1968) 2–17.

[7] T.H. Bauer, A general analytical approach toward the thermal conductivity of porous media, Int. J. Heat Mass Transfer 36 (1993) 4181–4191.

[8] E.E. Gonzo, Estimating correlations for the effective thermal conductivity of granular materials, Chem. Eng. J. 90 (2002) 299–302.

[9] J. Francl, W.D. Kingery, Thermal conductivity: IX, Experimental investigation of effect of porosity on thermal conductivity, J. Am. Ceram. Soc. 37 (1954) 99–107.

[10] I.H. Tavman, Effective thermal conductivity of granular porous materials, Int. Commun. Heat Mass Transfer 23 (1996) 169–176.

[11] G.C.J. Bart, Thermal Conduction in Non Homogeneous and Phase Change Media, Thesis, Delft University of Technology, Netherlands, 1994.

[12] Z. Hashin, S. Shtrikman, A variational approach to the theory of the effective magnetic permeability of multiphase materials, J. Appl. Phys. 33 (1962) 3125–3131.

[13] J.C. Maxwell, A Treatise on Electricity and Magnetism, third ed., Dover Publications Inc., New York, 1954, Reprint.

[14] R. Landauer, The electrical resistance of binary metallic mixtures, J. Appl. Phys. 23 (1952) 779–784.

[15] S. Kirkpatrick, Percolation and conduction, Rev. Mod. Phys. 45 (1973) 574–588.

[16] H.T. Davis, L.R. Valencourt, C.E. Johnson, Transport processes in composite media, J. Am. Ceram. Soc. 58 (1975) 446–452.

[17] W. Woodside, J.H. Messmer, Thermal conductivity of porous media. I. Unconsolidated sands, J. Appl. Phys. 32 (1961) 1688–1699.

[18] W. Woodside, J.H. Messmer, Thermal conductivity of porous media. II. Consolidated rocks, J. Appl. Phys. 32 (1961) 1699–1706.

[19] A. Sugawara, Y. Yoshizawa, An experimental investigation on the thermal conductivity of consolidated porous materials and its application to porous rock, Aust. J. Phys. 14 (1961) 469.

[20] J.K. Carson, S.J. Lovatt, D.J. Tanner, A.C. Cleland, Experimental measurements of the effective thermal conductivity of a pseudo-porous food analogue over a range of porosities and mean pore sizes, J. Food Eng. 63 (2004) 87–95.

[21] V.V. Calmidi, R.L. Mahajan, The effective thermal conductive of high porosity fibrous metal foams, ASME J. Heat Transfer 121 (1999) 466–471.

[22] X. Fu, R. Viskanta, J.P. Gore, Prediction of effective thermal conductivity of cellular ceramics, Int. Commun. Heat Mass Transfer 25 (1998) 151–160.

[24] R.L. Hamilton, O.K. Crosser, Thermal conductivity of heterogeneous two-component systems, Ind. Eng. Chem. Fundam. 1 (1962) 187–191.

[25] S.C. Cheng, R.I. Vachon, Prediction of thermal conductivity of two and three phase solid heterogeneous mixtures, Int. J. Heat Mass Transfer 12 (1969) 249–264.

[26] K. Boomsma, D. Poulikakos, On the effective thermal conductivity of a three-dimensionally structured fluid-saturated metal foam, Int. J. Heat Mass Transfer 44 (2001) 827–836.

[27] J.K. Carson, S.J. Lovatt, D.J. Tanner, A.C. Cleland, An analysis of the influence of material structure on the effective thermal conductivity of porous materials using finite element simulations, Int. J. Refrig. 26 (2003) 873–880.

[28] D. Kunii, J.M. Smith, Heat transfer in porous rocks, AIChE J. 3 (1960) 373–381.

[29] I. Nozad, R.G. Carbonell, S. Whitaker, Heat conduction in multiphase systems—I: Theory and experiment for two-phase systems, Chem. Eng. Sci. 40 (1985) 843–855.